

# A Phenomenological Organization of BCS Superconductivity via Fermion–Boson Duality: From an Occupation-Probability Decomposition to the Pseudogap and the BCS–BEC Crossover

*A readable phenomenological reformulation of superconductivity via  
Fermion–Boson Duality<sup>★</sup>*

Hirokazu Maruyama<sup>a,\*</sup>

<sup>a</sup>*Independent Researcher, Kobe, Japan*

---

## Abstract

The starting point of this paper is the Mühlischlegel formula  $\Delta(T)/\Delta_0 \simeq \tanh\{1.74 \sqrt{T_c/T - 1}\}$ , which closely approximates the weak-coupling BCS gap. By an elementary identity, the tanh in this formula can be written exactly as the difference of two complementary logistic occupation probabilities. Hence, at least within the range of this approximation, the BCS gap can be read as the difference between the B-type occupation probability  $L_B^{(e)}$  and the F-type occupation probability  $L_F^{(e)}$  of the electron sector, i.e. as  $L_B^{(e)} - L_F^{(e)}$ . Here the B-type component behaves bosonically, like a Cooper pair, while the F-type component represents the ordinary quasiparticle-like component.

Taking this mathematical fact as a core, we extend the phenomenology of Fermion–Boson Duality (FBD) step by step. First, in addition to the electron sector we introduce a gauge sector, and represent superconductivity through the four occupation probabilities  $\{L_B^{(e)}, L_F^{(e)}, L_B^{(\gamma)}, L_F^{(\gamma)}\}$ . When the transition centers of the electron and gauge sides coincide, the usual single-step transition of weak-coupling BCS is recovered. When the two separate, a staircase structure  $1 \rightarrow 1/2 \rightarrow 0$  appears in the observed gap, which becomes a candidate for describing the pseudogap of high-temperature superconductivity. Furthermore, we organize the case in which the tanh arguments of the two sectors have opposite signs as a competing structure, and represent the BCS–BEC crossover of cold-atom systems as a mixture of BCS-like and BEC-like occupation probabilities. In particular, the Bertsch parameter at the unitary point can be interpreted, in the language of FBD, as the admixture fraction of BCS character.

What is rigorous in this paper is the part in which the tanh of the Mühlischlegel approximation is decomposed into an occupation-probability difference. The reduction to four degrees of freedom, the averaging of the observed gap, the connection to the Matsubara scale, and the interpolation to BCS–BEC are phenomenological hypotheses to be tested against experiment.

**Keywords:** BCS theory, BCS–BEC crossover, Hill–Wheeler function,

## 1. Introduction: What is claimed, and how far

### 1.1. The central idea

In BCS theory [1], superconductivity is described as the formation of Cooper pairs. The finite-temperature gap  $\Delta(T)$  is determined by the gap equation, but in general it cannot be written in a simple closed form. For practical purposes, therefore, the Mühlischlegel approximation [2]

$$\frac{\Delta(T)}{\Delta_0} \simeq \tanh\left(1.74 \sqrt{\frac{T_c}{T} - 1}\right) \quad (1)$$

is widely used. Here  $\Delta_0 = \Delta(0) \simeq 1.764 k_B T_c$  is the zero-temperature gap and  $T_c$  is the transition temperature.

The first claim of this paper is the simple point that reading the tanh in Eq. (1) as “the difference of two occupation probabilities” clarifies the picture of the superconducting transition. That is, at low temperature the B-type (Cooper-pair-like) component dominates, and at  $T = T_c$  the B-type and F-type (quasiparticle-like) components become equal. This reinterpretation follows from an identity contained inside the Mühlischlegel approximation.

The second claim is the phenomenological proposal that, by extending this occupation-probability decomposition to the two-sector structure of Fermion–Boson Duality (FBD) [3], weak-coupling BCS, the pseudogap of high-temperature superconductivity, and the BCS–BEC crossover can be organized in the same mathematical language. The line of reasoning is summarized in Fig. 1.

### 1.2. The rigorous part and the hypothetical part

So that first-time readers are not confused, we separate the claims of this paper into “rigorous rewritings” and “phenomenological hypotheses.” Table 1 shows the overall placement.

Thus, this paper does not provide a new exact solution of the BCS gap equation. What is rigorous is the decomposition of the tanh contained in the existing approximation. On top of that, we build a physical picture in the language of FBD and propose relations that can be tested experimentally.

---

\*Revised version: May 31, 2026.

\*Corresponding author. ORCID: 0009-0004-3158-4827.

Email address: etctransformation@jcom.zaq.ne.jp (Hirokazu Maruyama)

Reading guide: build the core from an identity, then add hypotheses one at a time to widen the scope

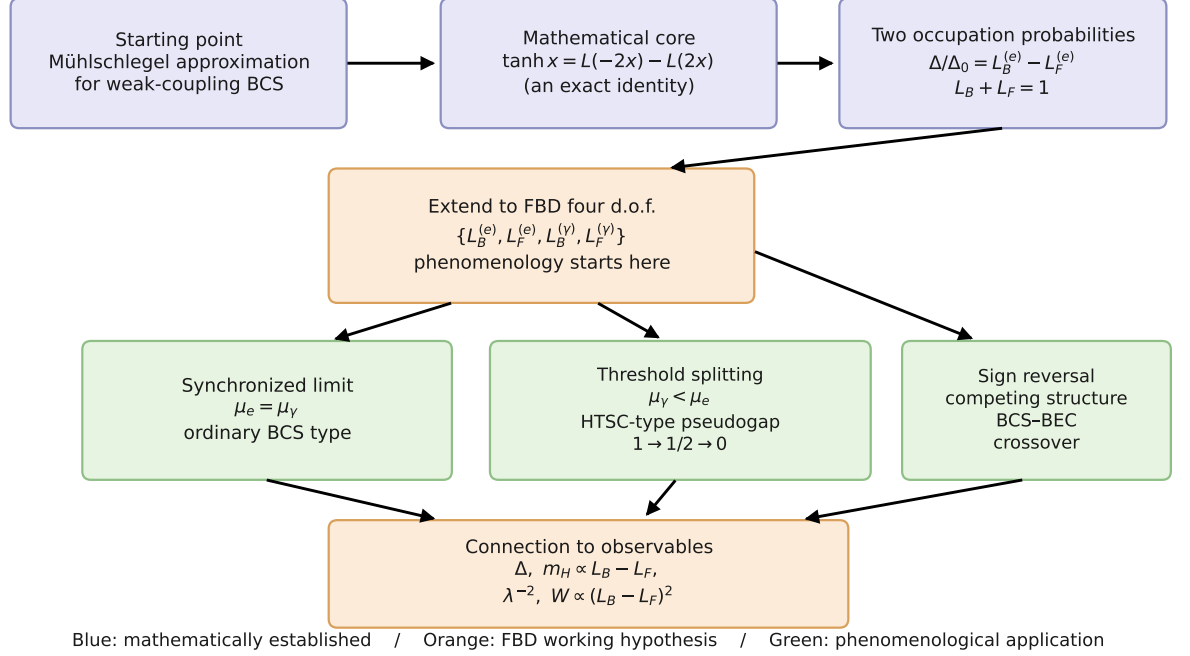


**Figure 1:** The line of reasoning of this paper. First, from the tanh identity, the weak-coupling BCS gap is read as the difference of two occupation probabilities. Up to this point it is a mathematical rewriting of the Mühschlegel approximation. After that, the formalism is extended to the four FBD degrees of freedom, and the three cases of the synchronized limit, threshold separation, and sign reversal are considered in turn.

### 1.3. The meaning of the B-type and F-type occupation probabilities

The “B-type” and “F-type” used repeatedly in this paper do not mean that the particles themselves are converted into bosons or fermions. They constitute a phenomenological classification in which the effective degrees of freedom of each sector are read as a bosonically behaving component (B-type) and a fermionically behaving component (F-type). In the context of superconductivity the correspondence is as follows.

- In the electron, or matter, sector,  $L_B^{(e)}$  represents the component that behaves bosonically, like a Cooper pair, and  $L_F^{(e)}$  represents the ordinary quasiparticle-like component.
- In the photon, or gauge, sector,  $L_B^{(\gamma)}$  represents the component that behaves with a mass, as in the Meissner state, and  $L_F^{(\gamma)}$  represents the component that behaves like an ordinary Maxwell photon.

**Table 1:** Classification of the claims of this paper by level.

Item	Content	Status
tanh decomposition	Write $\tanh x$ as the difference of two logistic functions.	Identity of elementary functions. Not an approximation.
Restatement of weak-coupling BCS	Read the Mühlischlegel approximation as $L_B^{(e)} - L_F^{(e)}$ .	An exact alternative expression within the range of the Mühlischlegel approximation.
FBD four degrees of freedom	Split the electron sector and the gauge sector each into B-type and F-type.	Phenomenological extension based on FBD.
Observed gap	Set it as a weighted average of the electron-side and gauge-side gaps.	Working hypothesis. The weights may depend on the measurement method and material.
HTSC pseudogap	Obtain a staircase gap $1 \rightarrow 1/2 \rightarrow 0$ via $\mu_\gamma < \mu_e$ .	Candidate model to be tested by comparison with experiment.
BCS–BEC crossover	Interpolate $\mu(g)$ by a mixture of BCS-like and BEC-like occupation probabilities.	Phenomenological application to cold-atom systems.

For each sector we assume the complementarity law

$$L_B^{(e)} + L_F^{(e)} = 1, \quad L_B^{(\gamma)} + L_F^{(\gamma)} = 1 \quad (2)$$

This is the normalization condition that “the total occupation probability is conserved,” and it corresponds to  $n_s/n + n_n/n = 1$  in the Gorter–Casimir two-fluid model [4].

## 2. The mathematical core: splitting tanh into two occupation probabilities

### 2.1. An identity for the logistic pair

The core of the argument is the following two logistic functions:

$$L_B(u) = \frac{1}{1 + e^{-u}}, \quad L_F(u) = \frac{1}{1 + e^{+u}}. \quad (3)$$

These two always satisfy

$$L_B(u) + L_F(u) = 1 \quad (4)$$

and, taking their difference,

$$L_B(u) - L_F(u) = \frac{e^u - 1}{e^u + 1} = \tanh\left(\frac{u}{2}\right) \quad (5)$$

Equation (5) is an identity, not an approximation. This equation is the smallest unit of the entire paper.

Physically, we read  $L_B$  and  $L_F$  as “two complementary occupation probabilities.” The difference  $L_B - L_F$  is the strength of order, expressing by how much the B-type component prevails over the F-type component.

## 2.2. Application to the Mühlischlegel approximation

Introducing

$$u(T) = 3.48 \sqrt{\frac{T_c}{T} - 1} \quad (6)$$

into Eq. (1), we have  $1.74 \sqrt{T_c/T - 1} = u(T)/2$ . Therefore, Eq. (1) can be written as

$$\frac{\Delta(T)}{\Delta_0} = L_B^{(e)}(T) - L_F^{(e)}(T) \quad (7)$$

where

$$L_B^{(e)}(T) = \frac{1}{1 + \exp[-u(T)]}, \quad (8)$$

$$L_F^{(e)}(T) = \frac{1}{1 + \exp[+u(T)]} \quad (9)$$

The complementarity law

$$L_B^{(e)}(T) + L_F^{(e)}(T) = 1 \quad (10)$$

also holds simultaneously.

What is important here is that Eq. (7) is not a new exact solution of the BCS gap equation, but an alternative expression of the Mühlischlegel approximation. Nonetheless, this alternative expression provides the lucid physical picture that “the gap is the difference between the B-type and F-type components.” This occupation-probability decomposition is shown in Fig. 2.

## 2.3. Reinterpretation of $T_c$

At  $T = T_c$  we have  $u(T) = 0$ , so

$$L_B^{(e)}(T_c) = L_F^{(e)}(T_c) = \frac{1}{2} \quad (11)$$

On the other hand, as  $T \rightarrow 0$  we have  $u(T) \rightarrow \infty$ , so

$$L_B^{(e)}(0) \rightarrow 1, \quad L_F^{(e)}(0) \rightarrow 0. \quad (12)$$

Therefore, at low temperature the Cooper-pair-like B-type component dominates, and as the temperature is raised the F-type quasiparticle component increases.  $T_c$  can be read as the temperature at which the nontrivial gap solution disappears and, at the same time, as the occupation-balance point at which the B-type and F-type components become equal.

## 2.4. Why this two-component representation alone is not enough

Equation (7) represents the temperature dependence of weak-coupling BCS lucidly. However, this two-component representation alone has difficulty describing the following phenomena.

- Because there is only one transition center, the gap closes as a single-step transition  $1 \rightarrow 0$ .

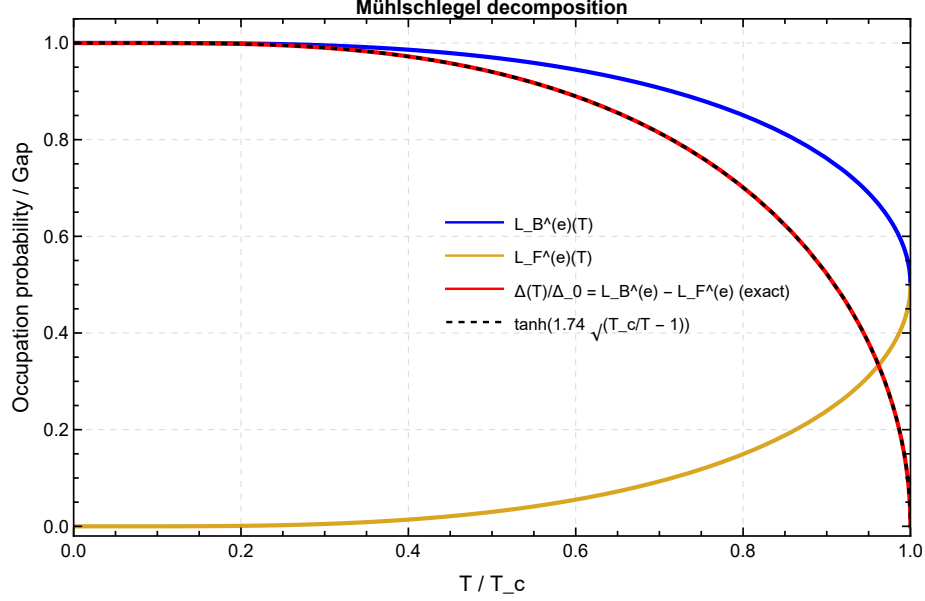


**Figure 2:** Occupation-probability decomposition of the Mühlischlegel approximation. The blue curve is the B-type occupation probability  $L_B^{(e)}(T)$ , the yellow curve is the F-type occupation probability  $L_F^{(e)}(T)$ , and the red curve is the difference  $L_B^{(e)}(T) - L_F^{(e)}(T)$ . The black dotted curve is the original Mühlischlegel approximation. The agreement between the red curve and the black dotted curve follows from the identity (5).

- It does not naturally include the phenomenon, observed in high-temperature superconductors, in which a partial gap remains in the temperature region above  $T_c$ , as in the pseudogap [5].

To remedy this insufficiency, in the next section we introduce a gauge sector independently, in addition to the electron sector.

### 3. The FBD four-degree-of-freedom model

#### 3.1. The electron sector and the gauge sector

In the FBD viewpoint, the electron and the photon are each split into B-type and F-type. In the phenomenology of superconductivity, we treat these as the four occupation probabilities

$$\{L_B^{(e)}, L_F^{(e)}, L_B^{(\gamma)}, L_F^{(\gamma)}\} \quad (13)$$

The correspondence is shown in Fig. 3.

The principal symbols are summarized in Table 2.

#### 3.2. A unified representation via the effective control parameter $E$

In Sec. 2 the occupation probabilities were written as functions of temperature  $T$ . From here, so that the same formalism can be used not only for temperature but also for

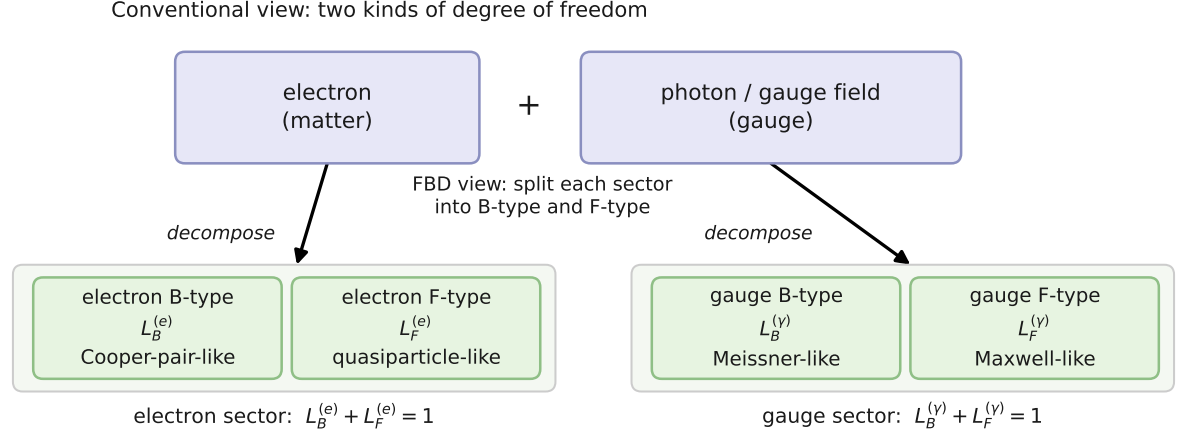


**Figure 3:** Schematic of the FBD four degrees of freedom. In the conventional description, two kinds of object are treated: the electron and the photon/gauge field. In FBD, each is split into B-type and F-type, so an electron sector ( $L_B^{(e)}, L_F^{(e)}$ ) and a gauge sector ( $L_B^{(\gamma)}, L_F^{(\gamma)}$ ) appear.

**Table 2:** Principal symbols used in this paper.

Symbol	Meaning
$L_B^{(e)}, L_F^{(e)}$	B-type and F-type occupation probabilities of the electron, or matter, sector. The weak-coupling BCS gap is written as $L_B^{(e)} - L_F^{(e)}$ .
$L_B^{(\gamma)}, L_F^{(\gamma)}$	B-type and F-type occupation probabilities of the photon, or gauge, sector. Introduced as the components representing the Meissner response and the effective mass acquisition of the gauge field.
$E$	An effective control parameter combining temperature, doping, excitation energy, and so on. In this paper it is defined so that larger $E$ proceeds toward the normal side.
$\mu_e, \mu_\gamma$	Transition centers of the electron sector and the gauge sector. At $E = \mu$ , the B-type and F-type of that sector become equal.
$\beta_e, \beta_\gamma$	Sharpness of the transition of each sector. Larger values make the switching steeper.
$\Delta_e, \Delta_\gamma$	Gaps of the electron sector and the gauge sector.
$\Delta_{\text{obs}}$	The effective gap seen in experiment. In the minimal model of this paper it is set as the average of $\Delta_e$ and $\Delta_\gamma$ .
$g = 1/(k_F a)$	The dimensionless coupling used in the BCS–BEC crossover. $a$ is the scattering length and $k_F$ is the Fermi wavenumber.
$L_F^{(\text{BCS})}, L_B^{(\text{BEC})}$	Effective occupation probabilities of BCS character and BEC character in the BCS–BEC crossover. In the minimal model $L_F^{(\text{BCS})} + L_B^{(\text{BEC})} = 1$ .

doping and coupling strength, we introduce an effective control parameter  $E$ . Depending on the context,  $E$  can be interpreted as  $k_B T$ , an excitation energy, or a composite quantity of temperature and doping. In this paper we adopt the convention that larger

$E$  proceeds toward the normal side.

For sector  $s = e, \gamma$  we define

$$u_s(E) = \beta_s(\mu_s - E) \quad (14)$$

and set the occupation probabilities as

$$L_B^{(s)}(E) = \frac{1}{1 + \exp[-u_s(E)]}, \quad (15)$$

$$L_F^{(s)}(E) = \frac{1}{1 + \exp[+u_s(E)]} \quad (16)$$

In this notation, the B-type dominates for  $E < \mu_s$  and the F-type dominates for  $E > \mu_s$ . Moreover

$$L_B^{(s)} + L_F^{(s)} = 1, \quad L_B^{(s)} - L_F^{(s)} = \tanh\left[\frac{\beta_s(\mu_s - E)}{2}\right] \quad (17)$$

holds. Using the fact that the Hill–Wheeler formula [6, 7] and a Fermi–Dirac-type logistic function have the same mathematical form, in this paper we use Eqs. (15)–(16) as the occupation probabilities of each sector.

### 3.3. Sector gaps and the observed gap

We define the normalized gap of each sector as

$$\delta_s(E) \equiv \frac{\Delta_s(E)}{\Delta_{s,0}} = \left[ L_B^{(s)}(E) - L_F^{(s)}(E) \right]_+, \quad s = e, \gamma \quad (18)$$

Here  $[x]_+ \equiv \max\{x, 0\}$  is the notation used so that, even when the occupation-probability difference becomes negative on the normal side, the gap is treated as 0.

The observed effective gap can, most generally, be written as

$$\frac{\Delta_{\text{obs}}(E)}{\Delta_0} = w_e \delta_e(E) + w_\gamma \delta_\gamma(E), \quad w_e + w_\gamma = 1 \quad (19)$$

The weights  $w_e, w_\gamma$  may vary with the material and the measurement method. In the minimal model of this paper we treat the electron side and the gauge side on an equal footing and adopt

$$\boxed{\frac{\Delta_{\text{obs}}(E)}{\Delta_0} = \frac{1}{2} [\delta_e(E) + \delta_\gamma(E)]} \quad (20)$$

Equation (20) is a working hypothesis, and estimating the weights of Eq. (19) by fitting to experimental data is a natural extension for the future.

### 3.4. The synchronized limit: ordinary weak-coupling BCS

We consider the limit in which the electron sector and the gauge sector make their transitions at the same timing. In this paper we call this the Anderson–Higgs strict ansatz, or the strong synchronization assumption. This is the simplest assumption,



namely that Cooper-pair formation and the Meissner effect occur simultaneously as the two faces of the Anderson–Higgs mechanism [8, 9]. In formulas,

$$\beta_e = \beta_\gamma, \quad \mu_e = \mu_\gamma \quad (21)$$

In this case

$$L_B^{(e)}(E) = L_B^{(\gamma)}(E), \quad L_F^{(e)}(E) = L_F^{(\gamma)}(E) \quad (22)$$

holds, and  $\delta_e(E) = \delta_\gamma(E)$  follows. Therefore, the average in Eq. (20) becomes the common value itself, and we obtain

$$\frac{\Delta_{\text{obs}}(E)}{\Delta_0} = L_B^{(e)}(E) - L_F^{(e)}(E) \quad (23)$$

This is the same as the weak-coupling BCS form of Sec. 2. That is, ordinary BCS is positioned as the synchronized limit of the FBD four-degree-of-freedom model.

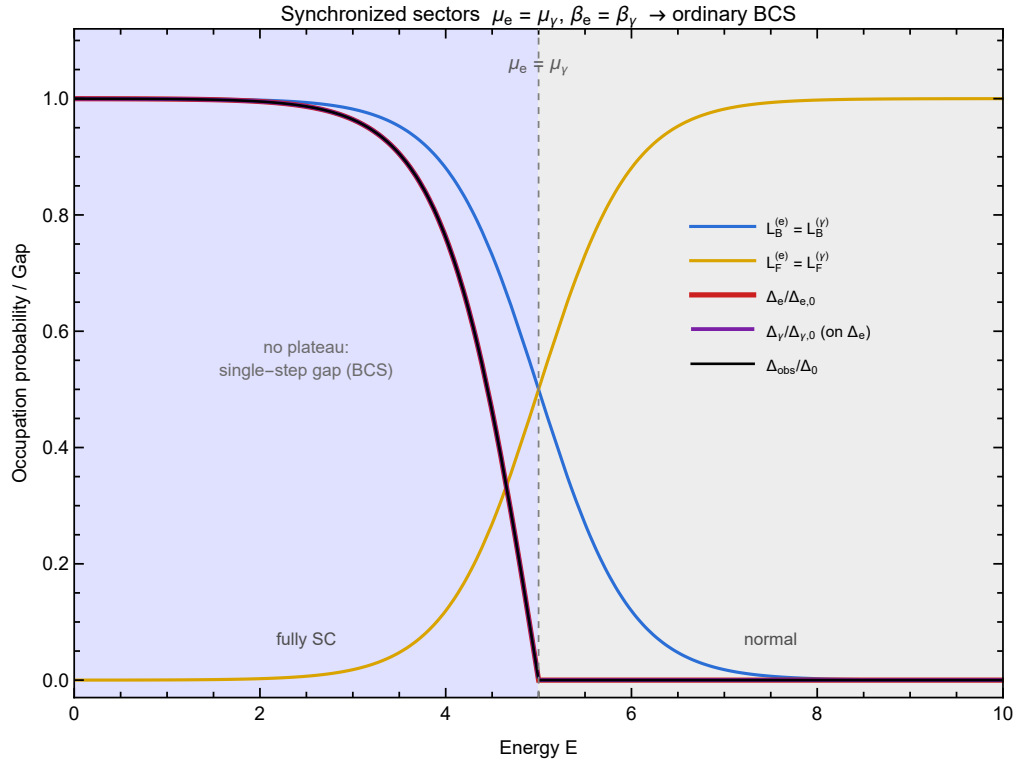


**Figure 4:** Occupation probabilities and gap in the synchronized limit (Eq. (21):  $\beta_e = \beta_\gamma, \mu_e = \mu_\gamma$ ). Because the two sectors coincide completely, we have  $L_B^{(e)} = L_B^{(\gamma)}, L_F^{(e)} = L_F^{(\gamma)}$ , and from  $\delta_e = \delta_\gamma$  the observed gap becomes the common value itself, as in Eq. (23). It is a single-step gap that opens for  $E < \mu$  and closes for  $E > \mu$ , and no plateau such as that in Sec. 4 (Fig. 5) appears. That is, ordinary weak-coupling BCS is reproduced as the synchronized limit of the FBD four-degree-of-freedom model.

That is, ordinary BCS is positioned as the synchronized limit of the FBD four-degree-of-freedom model (Fig. 4).

#### 4. Threshold separation: a candidate for the HTSC-type pseudogap

##### 4.1. Why a plateau appears

In high-temperature superconductors, part of the spectrum can retain a gap even in the region above the superconducting transition temperature. This region is called the pseudogap [5]. In the FBD four-degree-of-freedom model, the pseudogap arises from a shift between the transition centers of the electron sector and the gauge sector.

In particular, consider

$$\mu_\gamma < \mu_e \quad (24)$$

As  $E$  increases, the gauge-sector gap closes first at  $E = \mu_\gamma$ . However, the electron-sector gap remains up to  $E = \mu_e$ . Therefore, in the intermediate region

$$\mu_\gamma < E < \mu_e \quad (25)$$

only one of the sectors is active. In the minimal model (20), a plateau

$$\frac{\Delta_{\text{obs}}}{\Delta_0} \simeq \frac{1}{2} \quad (26)$$

appears in this region (Fig. 5).

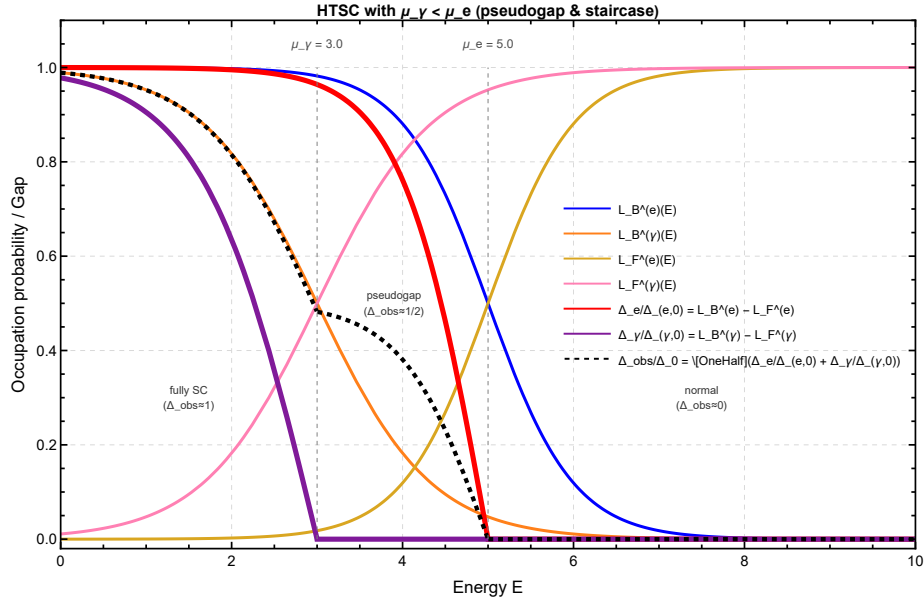


**Figure 5:** Conceptual diagram of the HTSC-type pseudogap due to threshold separation. As an example we use  $(\beta_e, \mu_e) = (2.0, 5.0)$ ,  $(\beta_\gamma, \mu_\gamma) = (1.5, 3.0)$ . The red curve is the electron-sector gap, the purple curve is the gauge-sector gap, and the black dotted curve is the observed gap from Eq. (20). For  $E < \mu_\gamma$  both sectors are open and  $\Delta_{\text{obs}}/\Delta_0 \simeq 1$ ; for  $\mu_\gamma < E < \mu_e$  only one remains and it is  $\simeq 1/2$ ; for  $E > \mu_e$  both close and it becomes 0.

In this way, the gap that closes in a single step in weak-coupling BCS becomes, through threshold separation, a staircase structure

$$1 \longrightarrow \frac{1}{2} \longrightarrow 0 \quad (27)$$

In the limit  $\mu_\gamma \rightarrow \mu_e$  the intermediate step disappears and the ordinary BCS-type single-step transition is recovered.

#### 4.2. Organizing synchronization and separation

Viewed in the FBD four-degree-of-freedom model, weak-coupling BCS and the HTSC-type pseudogap need not be expressed by separate formulas. The two can be organized as the difference of whether  $\mu_e$  and  $\mu_\gamma$  coincide or separate. This is summarized in Table 3.

### 5. Two-sector structure revealed by signs: cooperative and competing

#### 5.1. Same sign means cooperative, opposite sign means competing

In Secs. 3–4 we considered the case in which the electron sector and the gauge sector vary in the same direction. That is, the differences of the two sectors have the same-sign form

$$\delta_e \sim \tanh\left[\frac{\beta_e(\mu_e - E)}{2}\right], \quad \delta_\gamma \sim \tanh\left[\frac{\beta_\gamma(\mu_\gamma - E)}{2}\right] \quad (28)$$

Because the two switch on and off in the same direction, in this paper we call this a *cooperative* structure. The staircase structure of the HTSC-type pseudogap appears when the thresholds separate within this cooperative structure.

On the other hand, the case in which the two sectors are activated in opposite directions can also be considered. For example, in

$$\delta_{\text{BCS}}(E) \sim \tanh\left[\frac{\beta_{\text{BCS}}(\mu_{\text{BCS}} - E)}{2}\right], \quad (29)$$

$$\delta_{\text{BEC}}(E) \sim \tanh\left[\frac{\beta_{\text{BEC}}(E - \mu_{\text{BEC}})}{2}\right] \quad (30)$$

the argument of the second sector is reversed. In this case, because the BCS-like component and the BEC-like component rise from opposite directions, a V-shaped or smooth crossover appears in the intermediate region. In this paper we call this a *competing* structure. The difference between the two is shown in Fig. 6.

#### 5.2. Correspondence to the BCS–BEC crossover

A natural application of the competing structure is the BCS–BEC crossover in cold-atom systems [10–13]. This has been realized in cold-atom experiments using Feshbach resonance [14–16]. Using a Feshbach resonance, the effective attraction between fermions can be varied continuously. For weak attraction one obtains loosely bound,

**Table 3:** Organization of BCS-type and HTSC-type behavior by the FBD four-degree-of-freedom model.

Regime	Threshold relation	Observed gap
Weak-coupling BCS type	$\mu_e = \mu_\gamma$	The electron sector and the gauge sector are synchronized, and it appears as the usual single-step transition.
HTSC-type pseudo-gap	$\mu_\gamma < \mu_e$	The gauge sector closes first, and an intermediate region in which only the electron sector remains appears. In the minimal model $\Delta_{\text{obs}}/\Delta_0 \simeq 1/2$ .
Reverse threshold separation	$\mu_e < \mu_\gamma$	The electron sector closes first, leaving a separated state in which only the gauge side remains. It is not the main object of this paper, but can be considered as a measurement-probe-dependent anomalous response.

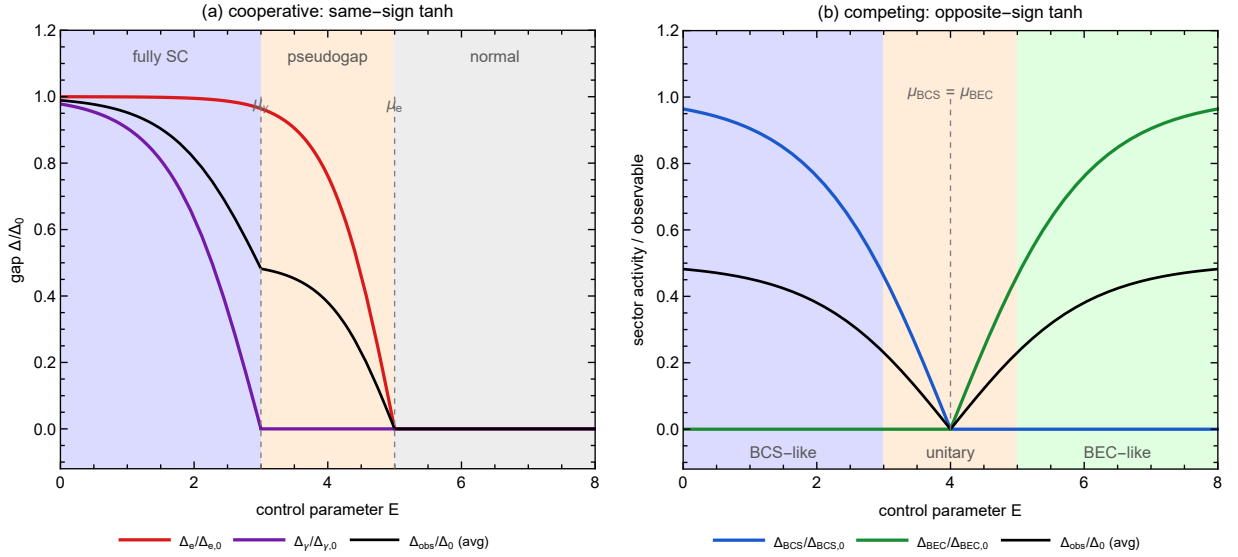


**Figure 6:** Sign classification of the two-sector structure. In the cooperative structure on the left, the tanh arguments of the two sectors have the same sign, and the observed gap varies in a staircase. In the competing structure on the right, the arguments of the two sectors have opposite signs, and a V-shaped crossover structure appears in the intermediate region.

large Cooper pairs (BCS side), and for strong attraction one obtains a condensate of small, tightly bound molecules (BEC side). What is important is that this change is a smooth crossover rather than a phase transition.

In cold-atom systems, the control variable used is

$$g = \frac{1}{k_F a} \quad (31)$$

where  $a$  is the scattering length and  $k_F$  is the Fermi wavenumber.  $g < 0$  corresponds to the BCS side,  $g = 0$  to the unitary point, and  $g > 0$  to the BEC side. Figure 7 shows the correspondence between the general effective control parameter  $E$  and the concrete axis  $g$  of cold-atom systems.

In this section we specialize the control variable from the general effective control parameter  $E$  to the cold-atom coupling  $g = 1/(k_F a)$ . The correspondence of symbols is summarized in Table 4.

### 5.3. Chemical potential from the FBD mixture model

We represent the state midway through the crossover as a mixture of a BCS-like component and a BEC-like component. In the BCS limit we set

$$\mu_{\text{BCS}}^{\text{sat}} = +\epsilon_F \quad (32)$$

and in the BEC limit, as the contribution of deeply bound molecules, half of the two-body binding energy of a molecule  $\epsilon_b = \hbar^2/(ma^2)$  contributes to the chemical potential per particle. Normalizing by  $\epsilon_F = \hbar^2 k_F^2/(2m)$  gives  $\epsilon_b/\epsilon_F = 2g^2$ , so we use

$$\mu_{\text{BEC}}(g) = -\frac{\epsilon_b}{2} = -\frac{1}{(k_F a)^2} \epsilon_F = -g^2 \epsilon_F \quad (33)$$

Weighting the two by the BCS-character occupation probability  $L_F^{(\text{BCS})}(g)$  and the BEC-character occupation probability  $L_B^{(\text{BEC})}(g)$ , we obtain

$$\boxed{\frac{\mu(g)}{\epsilon_F} = L_F^{(\text{BCS})}(g) \cdot (+1) + L_B^{(\text{BEC})}(g) \cdot (-g^2)} \quad (34)$$

The complementarity law is

$$L_F^{(\text{BCS})}(g) + L_B^{(\text{BEC})}(g) = 1 \quad (35)$$

In the minimal model we set

$$L_B^{(\text{BEC})}(g) = \frac{1}{1 + \exp[-\beta_g(g - g_*)]}, \quad (36)$$

$$L_F^{(\text{BCS})}(g) = 1 - L_B^{(\text{BEC})}(g) \quad (37)$$

where  $\beta_g$  is the sharpness of the change and  $g_*$  is the center at which the system moves from BCS character to BEC character.

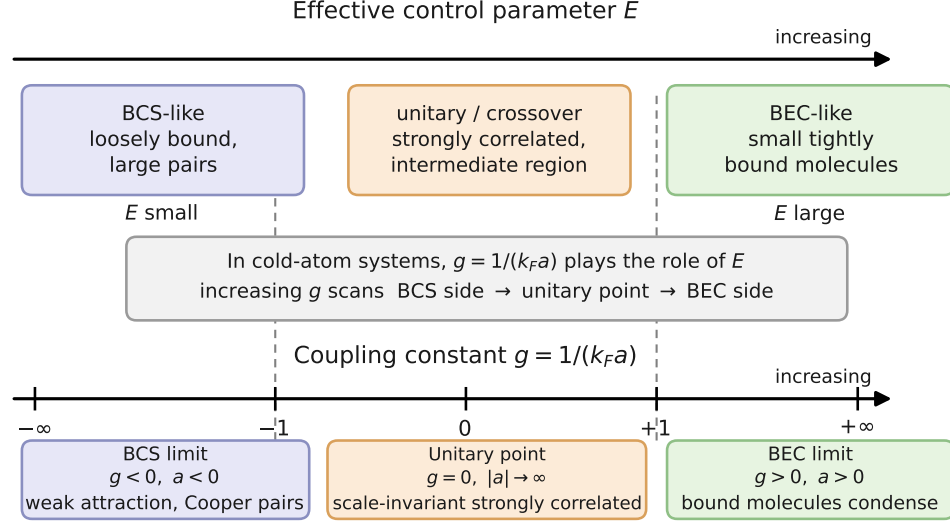


**Figure 7:** Correspondence between the effective control parameter  $E$  and the coupling constant  $g = 1/(k_F a)$  of cold-atom systems. As  $g$  increases, one proceeds from the BCS side through the unitary point to the BEC side.

**Table 4:** Variable correspondence between the general representation (Secs. 3–4) and the BCS–BEC crossover representation of this section. Both use the same logistic pair (Eqs. (3)–(5)), and the control variable, transition center, sharpness, and the two occupation probabilities are in one-to-one correspondence.

General representation (Secs. 3–4)	BCS–BEC (this section)	Meaning
$E$ (effective control parameter)	$g = 1/(k_F a)$	Control variable
$\mu_s$ (sector transition center)	$g_*$	Center where the two components become equal
$\beta_s$	$\beta_g$	Sharpness of the transition
$L_B^{(s)}, L_F^{(s)}$ (B-type / F-type)	$L_B^{(\text{BEC})}, L_F^{(\text{BCS})}$ (BEC character / BCS character)	The two complementary occupation probabilities

#### 5.4. FBD interpretation of the Bertsch parameter

At the unitary point  $g = 0$ , the BEC term of Eq. (34) vanishes because  $-g^2 = 0$ . Therefore

$$\xi_B \equiv \frac{\mu(0)}{\epsilon_F} = L_F^{(\text{BCS})}(0) \quad (38)$$

That is, the Bertsch parameter  $\xi_B$  [17] can be read, in the language of FBD, as the admixture fraction of BCS character at the unitary point.

Using the representative value  $\xi_B \approx 0.376$  [18] (consistent also with QMC calculations [19, 20]), we have

$$L_F^{(\text{BCS})}(0) = 0.376, \quad L_B^{(\text{BEC})}(0) = 0.624 \quad (39)$$

Substituting into Eq. (36) gives

$$\beta_g g_* = \ln\left(\frac{1}{0.624} - 1\right) \simeq -0.506 \quad (40)$$

For example, choosing  $\beta_g = 4$  gives  $g_* \simeq -0.127$ . A comparison of the  $\mu(g)$  curve using this  $(\beta_g, g_*) = (4.0, -0.127)$  with literature values from QMC and cold-atom experiments [18, 21] is shown in Fig. 8. Note that with this  $(\beta_g, g_*)$  the sign reversal of the chemical potential occurs at  $g_0 \simeq 0.37$ . If one wishes to match the experimental sign-reversal position ( $g \sim 0.4$ – $0.5$ ), one can keep  $\xi_B = 0.376$  (i.e.  $\beta_g g_* \simeq -0.506$ ) fixed and choose  $\beta_g$  somewhat smaller.

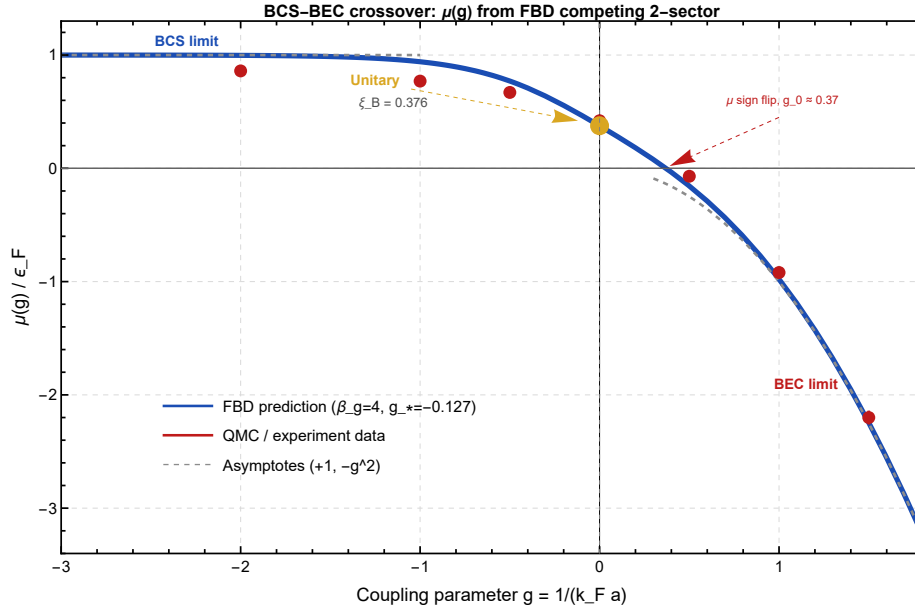


**Figure 8:** Chemical potential  $\mu(g)/\epsilon_F$  of the BCS–BEC crossover from the FBD competing two-sector structure. The blue solid curve is the FBD curve from Eq. (34), with  $(\beta_g, g_*) = (4.0, -0.127)$  and the unitary point matched to the experimental value  $\xi_B = 0.376$  [18]. The red circles are  $\mu/\epsilon_F$  evaluated from the analytic parametrization [22] of the QMC equation of state [21], which gives 0.42 at the unitary point. The gold point is the experimental unitary value  $\mu/\epsilon_F = \xi_B = 0.376$  of Ku et al. [18]. It connects to  $\mu \rightarrow +\epsilon_F$  as  $g \rightarrow -\infty$  and to  $\mu \rightarrow -g^2\epsilon_F = -\epsilon_F/(k_F a)^2$  as  $g \rightarrow +\infty$ .

The advantage of this interpretation is that the universal number  $\xi_B$  can be read as the probability of “how BCS-like the system is at the unitary point.” However, this is not a microscopic derivation but a phenomenology that interpolates the two limiting values by occupation probabilities. To describe the finite-temperature  $\mu(g, T)$  or  $T_c(g)$  [23], one needs to introduce a temperature dependence of  $\beta_g$  and  $g_*$ .

### 5.5. Summary of the three regimes

The discussion so far can be organized as in Table 5.

**Table 5:** The three regimes of the FBD two-sector structure.

Regime	Sector relation	Behavior of observables	Physical correspondence
Synchronized cooperative	Same sign, and $\mu_e = \mu_\gamma$	Closes in a single step $1 \rightarrow 0$	Weak-coupling BCS
Separated cooperative	Same sign, and $\mu_\gamma < \mu_e$	Staircase $1 \rightarrow 1/2 \rightarrow 0$	HTSC-type pseudogap candidate
Competing	Opposite sign	V-shaped, or smooth crossover	BCS–BEC crossover

## 6. Connection to experimental quantities

### 6.1. Connection to the Matsubara energy scale

In finite-temperature quantum field theory, the Matsubara frequencies provide an energy scale proportional to temperature [24]. The energy spacing between adjacent Matsubara frequencies is

$$2\pi k_B T \quad (41)$$

In this paper, as a connection hypothesis linking the characteristic energy that appears in the FBD decomposition to this temperature scale, we adopt

$$\hbar\omega_* = 2\pi k_B T \quad (42)$$

This is not a derived result but an ansatz for matching the FBD occupation-probability description to the standard temperature scale of finite-temperature field theory.

### 6.2. The Meissner penetration depth and spectral weight

The London penetration depth  $\lambda(T)$  represents the strength of the Meissner effect, and in general  $\lambda^{-2}(T)$  is proportional to the superfluid density. In the weak-coupling synchronized limit, since we read the amplitude of the order parameter as  $L_B^{(e)} - L_F^{(e)}$ , we assume

$$\frac{\lambda_0^2}{\lambda^2(T)} = [L_B^{(e)}(T) - L_F^{(e)}(T)]^2 = \left[ \frac{\Delta(T)}{\Delta_0} \right]^2 \quad (43)$$

That the exponent is 2 is consistent with the standard relation  $n_s \propto |\psi|^2$ . Near  $T_c$  we have  $\Delta \propto (1 - T/T_c)^{1/2}$ , so  $\lambda_0^2/\lambda^2 \propto 1 - T/T_c$ , which corresponds to the linear dependence of the superfluid density [25].

For the optical spectral weight as well, from the correspondence with the Ferrell–Glover–Tinkham sum rule [26, 27], we can write

$$\frac{W^{(\gamma)}(T)}{W^{(\gamma)}(0)} = [L_B^{(e)}(T) - L_F^{(e)}(T)]^2 \quad (44)$$



### 6.3. Relations testable on the same sample

Summarizing the above, in the weak-coupling synchronized limit the following relations are predicted:

$$\boxed{\begin{aligned}\frac{\Delta(T)}{\Delta_0} &= \frac{m_H(T)}{m_H(0)} = L_B^{(e)}(T) - L_F^{(e)}(T), \\ \frac{\lambda_0^2}{\lambda^2(T)} &= \frac{W^{(\gamma)}(T)}{W^{(\gamma)}(0)} = [L_B^{(e)}(T) - L_F^{(e)}(T)]^2.\end{aligned}} \quad (45)$$

Here  $m_H(T)$  is the effective mass of the Higgs, or amplitude, mode. In BCS the energy of the Higgs mode is proportional to  $2\Delta(T)$ , so it is expected to follow the same occupation-probability difference as the gap [28].

Equation (45) is testable. One measures, on the same sample, the gap by ARPES or STS, the penetration depth by  $\mu$ SR or infrared optics, and the Higgs mode by THz spectroscopy, and examines whether the gap and the Higgs mass are organized as  $L_B^{(e)} - L_F^{(e)}$  and the penetration depth and spectral weight as its square.

This difference between the first power and the second power is shown in Fig. 9. The dashed curve is  $\Delta/\Delta_0 = L_B^{(e)} - L_F^{(e)}$  (the same as the difference in Fig. 2), and the solid curve is its square. At low temperature the two are close, but near  $T_c$  the dashed curve falls steeply, whereas the solid curve vanishes linearly. By measuring the gap and the penetration depth on the same sample, one can verify Eq. (45) as this difference in shape.

## 7. Correspondence with existing superconductivity concepts

Mapping the FBD terminology onto existing superconductivity concepts, one can organize it as in Table 6. This is not a quantitative derivation but a dictionary for “rereading” well-known concepts of superconductivity in the language of FBD occupation probabilities. Each row places the conventional concept on the left, its standard view in the center, and the rereading of this paper on the right.

We illustrate the meaning of the rereadings in the table concretely with two representative examples (the amplitude of the order parameter and the phase of the Josephson effect).

**(1) Amplitude of the order parameter.** In Ginzburg–Landau theory the order parameter is written as  $\psi = |\psi|e^{i\phi}$ , with the amplitude  $|\psi|$  representing the strength of superconductivity and the phase  $\phi$  representing how the condensate is aligned. In this paper we read this amplitude as

$$|\psi(T)| \propto L_B^{(e)}(T) - L_F^{(e)}(T) \quad (46)$$

At  $T = T_c$  we have  $L_B^{(e)} = L_F^{(e)} = 1/2$ , so the right-hand side becomes zero and  $|\psi|$  vanishes. This is consistent with the fact that “superconductivity disappears at  $T_c$ .”

**(2) Phase of the Josephson effect.** Having read the amplitude as in Eq. (46), we next consider the phase  $\phi$ . The Josephson effect is the phenomenon in which, when two superconductors are connected, the phase difference  $\delta\phi$  of their respective condensates

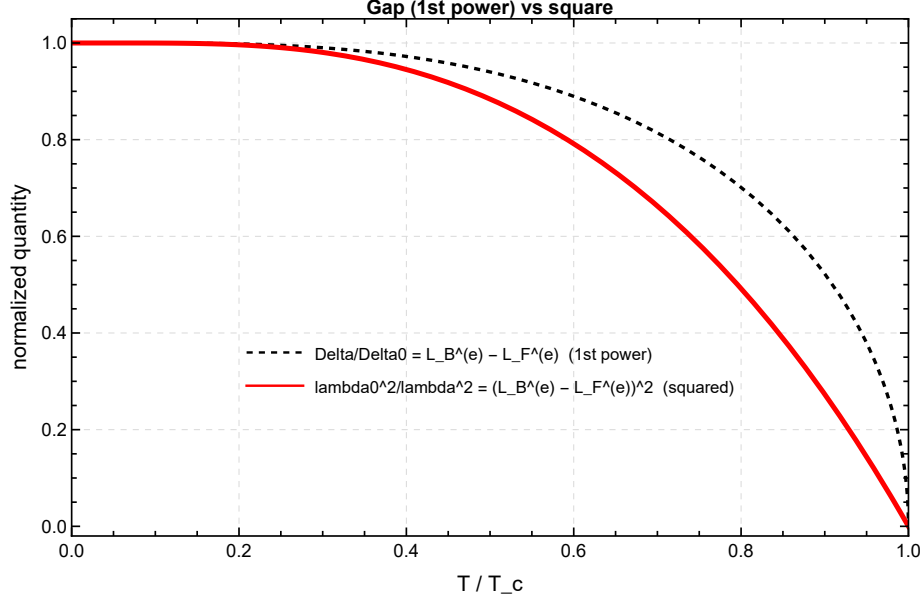


**Figure 9:** Temperature dependence of the first power and the second power in the weak-coupling synchronized limit. The dashed curve is the normalized gap  $\Delta/\Delta_0 = L_B^{(e)} - L_F^{(e)}$ , and the solid curve is its square, which is the curve followed by the inverse square of the penetration depth  $\lambda_0^2/\lambda^2$  and the spectral weight  $W^{(\gamma)}$  (Eq. (45)). Near  $T_c$  the dashed curve falls steeply, whereas the solid curve heads to zero linearly, proportional to  $1 - T/T_c$ .

(order parameters) produces a supercurrent  $I \propto \sin \delta\phi$  [30]. In this paper, since we read the phase of the order parameter as the internal phase carried by the B-type channel,  $\delta\phi$  corresponds to the phase difference of the B-type channels of the two superconductors. Furthermore, in the weak-coupling synchronized limit, inside each superconductor the B-type components of the electron side and the gauge side move aligned in the same direction (synchronized), so there is no need to treat the two phases for the electron and the gauge separately, and they can be combined into a single condensate phase. That is, the very fact that the sectors are synchronized is the premise for combining the phase into one and discussing the Josephson effect.

## 8. Conclusion and future tasks

In this paper, we have reread the Mühlischlegel approximation of weak-coupling BCS in the language of FBD occupation probabilities. The conclusions are summarized concisely.

1. By the tanh identity, the Mühlischlegel approximation can be written as  $\Delta(T)/\Delta_0 = L_B^{(e)}(T) - L_F^{(e)}(T)$ .
2.  $T = T_c$  can be read as the occupation-balance point at which  $L_B^{(e)} = L_F^{(e)} = 1/2$ .

**Table 6:** Correspondence between conventional superconductivity concepts and the FBD picture. The right column is not a quantitative derivation but a rereading to make the physical picture easier to read.

Conventional concept	Standard view	Rereading in FBD
Two-fluid model [4]	Split the electrons into a normal-fluid component and a superfluid component.	Take the normal fluid as $L_F^{(e)}$ and the superfluid as $L_B^{(e)}$ , and represent them by the complementarity law $L_B^{(e)} + L_F^{(e)} = 1$ .
Anderson–Higgs mechanism [8, 9]	The gauge field acquires a mass.	The gauge sector becomes B-type dominant and acquires a mass, occurring simultaneously with the Meissner response.
Meissner response	A superconducting response that expels magnetic field.	Read as the state in which $L_B^{(\gamma)}$ becomes dominant in the gauge sector.
Order parameter $\psi$	Represents the amplitude and phase of the condensate.	Read the amplitude as $L_B^{(e)} - L_F^{(e)}$ and the phase as the internal phase carried by the B-type channel.
Meaning of $T_c$	The temperature at which the nontrivial gap solution disappears.	The temperature at which $L_B^{(e)} = L_F^{(e)} = 1/2$ so that the difference vanishes (occupation-balance point).
Andreev reflection [29]	At a boundary an electron is reflected as a hole, and a Cooper pair enters the superconducting side.	Read as the process in which an F-type component is converted into a B-type component.
Pseudogap [5]	There are several views on its origin.	A candidate for separation due to a shift between the transition centers of the electron sector and the gauge sector ( $\mu_\gamma \neq \mu_e$ ).
Josephson effect [30]	The phase difference of two condensates produces a current.	The phase difference of the B-type channels of the two superconductors produces a current.
Type-I/II superconductivity	Distinguished by the magnitude of $\kappa = \lambda/\xi$ .	Read as the ratio $\kappa$ of the gauge-sector length $\lambda$ to the matter-sector length $\xi$ .

- Introducing the FBD four degrees of freedom  $\{L_B^{(e)}, L_F^{(e)}, L_B^{(\gamma)}, L_F^{(\gamma)}\}$  combining the electron sector and the gauge sector, weak-coupling BCS is positioned as the limit in which the two sectors are synchronized.
- Through the threshold separation  $\mu_\gamma < \mu_e$ , a staircase structure  $1 \rightarrow 1/2 \rightarrow 0$  appears in the observed gap, becoming a phenomenological candidate for the HTSC-type pseudogap.

5. If the tanh arguments of the two sectors have the same sign it is a cooperative structure, and if opposite signs a competing structure. The former corresponds to the HTSC-type pseudogap and the latter to the BCS–BEC crossover.
6. In the BCS–BEC crossover, the Bertsch parameter  $\xi_B$  at the unitary point can be interpreted as the admixture fraction of BCS character  $L_F^{(\text{BCS})}(0)$ .
7. We proposed the testable relation that the gap and the Higgs mode follow the occupation-probability difference  $L_B^{(e)} - L_F^{(e)}$ , while the Meissner penetration depth and the spectral weight follow its square.

Summarizing these, for each superconductor, once the transition center  $\mu_s$  and the sharpness  $\beta_s$  of each sector are estimated from the temperature or energy dependence of the gap, the behavior of the penetration depth, the spectral weight, and the Higgs mode is determined through Eq. (45) with no additional free parameters. Therefore, by examining whether these are consistent on the same sample, the predictive power and the limits of applicability of this framework can be tested material by material. In particular, in the case of the pseudogap with  $\mu_\gamma \neq \mu_e$  or the competing case,  $\beta_s, \mu_s$  are expected to take values specific to the material and to appear as differences in detailed behavior. On the other hand, for weak-coupling BCS the gap curve is nearly a universal form, so the differences from material to material are small.

A future task is to estimate  $\mu_e, \mu_\gamma, \beta_e, \beta_\gamma$  and the weights  $w_e, w_\gamma$  from data for individual materials and experimental systems. In particular, by comparing ARPES, STS,  $\mu$ SR, infrared optics, and THz spectroscopy on the same sample, the validity of Eq. (45) can be tested. For the BCS–BEC crossover, it is necessary to investigate how far the FBD occupation probabilities are valid not only for the  $T = 0$  chemical potential but also for the finite-temperature  $\mu(g, T)$ ,  $T_c(g)$ , momentum distribution, and pair correlation function.

## Acknowledgments

This research was carried out as independent research. The author thanks the researchers who provided discussion and advice during the formation of the FBD framework. This research received no specific funding.

## Appendix A. Mathematica script for figure generation

The Mathematica script for generating the numerical figures included in this paper (Figs. 2, 4, 5, 6, 8) is registered and publicly available on Zenodo.

H. Maruyama, “BCS\_figures: A Mathematica script for visualizing BCS superconducting gaps via the Fermion–Boson Duality framework,” Zenodo, version 3 (June 1, 2026).

DOI: 10.5281/zenodo.20481570

URL: <https://zenodo.org/records/20481570>

By running this script, the main numerical figures of this paper can be reproduced.

## Appendix B. Possibility of extension to other fields

The mathematical structure at the center of this paper is the writing of  $\tanh$  as the difference of two complementary logistic occupation probabilities. Similar sigmoidal or  $\tanh$  shapes also appear in mean-field-type phase transitions other than superconductivity. Therefore, the FBD occupation-probability decomposition may possibly be applied to systems such as the following.

- **Spontaneous magnetization of an Ising/Heisenberg ferromagnet:** In the mean-field approximation a self-consistent equation of the type  $m = \tanh[\beta(h + zJm)]$  appears. The magnetization becomes a candidate for being read as a B-type/F-type occupation-probability difference.
- **Spontaneous polarization of a ferroelectric:** The temperature dependence of the spontaneous polarization is sometimes expressed by a sigmoidal or  $\tanh$ -type empirical formula. It may possibly be organized as a complementarity law between polarization domains and a disordered component.
- **Superfluid He-4/He-3:** The two-fluid model directly corresponds to the complementarity law  $L_B + L_F = 1$  of this paper. The B-type can be read as the condensate component and the F-type as the excitation component.
- **Chiral condensate of QCD:** The disappearance of the chiral condensate in high-temperature QCD also appears, in the mean-field approximation, as a sigmoidal order parameter. It may possibly be organized as an occupation-probability difference between a condensate component and a symmetry-restoring component.

These are not the main conclusions of this paper but a prospect indicating that the same mathematical structure appears in other fields. The concrete B-type/F-type correspondences and whether an intermediate phase exists due to the threshold separation of multiple sectors are tasks to be tested individually in each field.

## References

- [1] J. Bardeen, L. N. Cooper, and J. R. Schrieffer, “Theory of Superconductivity,” *Phys. Rev.* **108**, 1175 (1957).
- [2] B. Mühschlegel, “Die thermodynamischen Funktionen des Supraleiters,” *Z. Physik* **155**, 313 (1959).
- [3] H. Maruyama, “Proposal for statistical mechanics-based UV regularization using fermion–boson transition functions,” *Frontiers in Physics* **13**, 1618853 (2025). doi:10.3389/fphy.2025.1618853.
- [4] C. J. Gorter and H. B. G. Casimir, “On Superconductivity I,” *Physica* **1**, 306 (1934).
- [5] T. Timusk and B. Statt, “The pseudogap in high-temperature superconductors: an experimental survey,” *Rep. Prog. Phys.* **62**, 61 (1999).

- [6] D. L. Hill and J. A. Wheeler, “Nuclear Constitution and the Interpretation of Fission Phenomena,” *Phys. Rev.* **89**, 1102 (1953).
- [7] H. Maruyama, “Application of the Hill–Wheeler Formula in Statistical Models of Nuclear Fission: A Statistical–Mechanical Approach Based on Similarities with Semiconductor Physics,” *Entropy* **27**, 227 (2025). doi:10.3390/e27030227.
- [8] P. W. Anderson, “Plasmons, Gauge Invariance, and Mass,” *Phys. Rev.* **130**, 439 (1963).
- [9] P. W. Higgs, “Broken Symmetries and the Masses of Gauge Bosons,” *Phys. Rev. Lett.* **13**, 508 (1964).
- [10] A. J. Leggett, “Diatomic molecules and Cooper pairs,” in *Modern Trends in the Theory of Condensed Matter*, Lecture Notes in Physics, vol. 115, Springer (1980), pp. 13–27.
- [11] P. Nozières and S. Schmitt-Rink, “Bose condensation in an attractive fermion gas: from weak to strong coupling superconductivity,” *J. Low Temp. Phys.* **59**, 195 (1985).
- [12] Q. Chen, J. Stajic, S. Tan, and K. Levin, “BCS–BEC crossover: From high temperature superconductors to ultracold superfluids,” *Phys. Rep.* **412**, 1 (2005).
- [13] M. Randeria and E. Taylor, “Crossover from Bardeen–Cooper–Schrieffer to Bose–Einstein Condensation and the Unitary Fermi Gas,” *Annu. Rev. Condens. Matter Phys.* **5**, 209 (2014).
- [14] C. A. Regal, M. Greiner, and S. D. Jin, “Observation of Resonance Condensation of Fermionic Atom Pairs,” *Phys. Rev. Lett.* **92**, 040403 (2004).
- [15] M. W. Zwierlein, J. R. Abo-Shaeer, A. Schirotzek, C. H. Schunck, and W. Ketterle, “Vortices and superfluidity in a strongly interacting Fermi gas,” *Nature* **435**, 1047 (2005).
- [16] M. Bartenstein, A. Altmeyer, S. Riedl, S. Jochim, C. Chin, J. H. Denschlag, and R. Grimm, “Crossover from a Molecular Bose–Einstein Condensate to a Degenerate Fermi Gas,” *Phys. Rev. Lett.* **92**, 120401 (2004).
- [17] G. F. Bertsch, MBX Challenge, in R. F. Bishop, K. A. Gernoth, and N. R. Walet (Eds.), *Recent Progress in Many-Body Theories*, World Scientific (2000).
- [18] M. J. H. Ku, A. T. Sommer, L. W. Cheuk, and M. W. Zwierlein, “Revealing the Superfluid Lambda Transition in the Universal Thermodynamics of a Unitary Fermi Gas,” *Science* **335**, 563 (2012).
- [19] J. Carlson and S. Reddy, “Asymmetric Two-Component Fermion Systems in Strong Coupling,” *Phys. Rev. Lett.* **95**, 060401 (2005).
- [20] S. Y. Chang and G. F. Bertsch, “Unitary Fermi gas in a harmonic trap,” *Phys. Rev. A* **76**, 021603(R) (2007).

- [21] G. E. Astrakharchik, J. Boronat, J. Casulleras, and S. Giorgini, “Equation of State of a Fermi Gas in the BEC-BCS Crossover: A Quantum Monte Carlo Study,” *Phys. Rev. Lett.* **93**, 200404 (2004).
- [22] N. Manini and L. Salasnich, *Bulk and collective properties of a dilute Fermi gas in the BCS–BEC crossover*, *Phys. Rev. A* **71**, 033625 (2005).
- [23] E. Burovski, N. Prokof’ev, B. Svistunov, and M. Troyer, “Critical Temperature and Thermodynamics of Attractive Fermions at Unitarity,” *Phys. Rev. Lett.* **96**, 160402 (2006).
- [24] T. Matsubara, “A New Approach to Quantum-Statistical Mechanics,” *Prog. Theor. Phys.* **14**, 351 (1955).
- [25] D. C. Mattis and J. Bardeen, “Theory of the Anomalous Skin Effect in Normal and Superconducting Metals,” *Phys. Rev.* **111**, 412 (1958).
- [26] R. A. Ferrell and R. E. Glover III, “Conductivity of Superconducting Films: A Sum Rule,” *Phys. Rev.* **109**, 1398 (1958).
- [27] M. Tinkham and R. A. Ferrell, “Determination of the Superconducting Skin Depth from the Energy Gap and Sum Rule,” *Phys. Rev. Lett.* **2**, 331 (1959).
- [28] R. Matsunaga, N. Tsuji, H. Fujita, A. Sugioka, K. Makise, Y. Uzawa, H. Terai, Z. Wang, H. Aoki, and R. Shimano, “Light-induced collective pseudospin precession resonating with Higgs mode in a superconductor,” *Science* **345**, 1145 (2014).
- [29] A. F. Andreev, “The Thermal Conductivity of the Intermediate State in Superconductors,” *Sov. Phys. JETP* **19**, 1228 (1964).
- [30] B. D. Josephson, “Possible new effects in superconductive tunnelling,” *Phys. Lett.* **1**, 251 (1962).